JUSTC

Article

http://justc.ustc.edu.cn

Received: October 01, 2022; Accepted: November 04, 2022

Molecular mechanism underlying ABC exporter gating: a computational study

Zi Wang, and Jielou Liao ✉

Department of Chemical Physics, University of Science and Technology of China, Hefei 230026, China

✉Correspondence: Jielou Liao, E-mail: liaojl@ustc.edu.cn

Graphical abstract

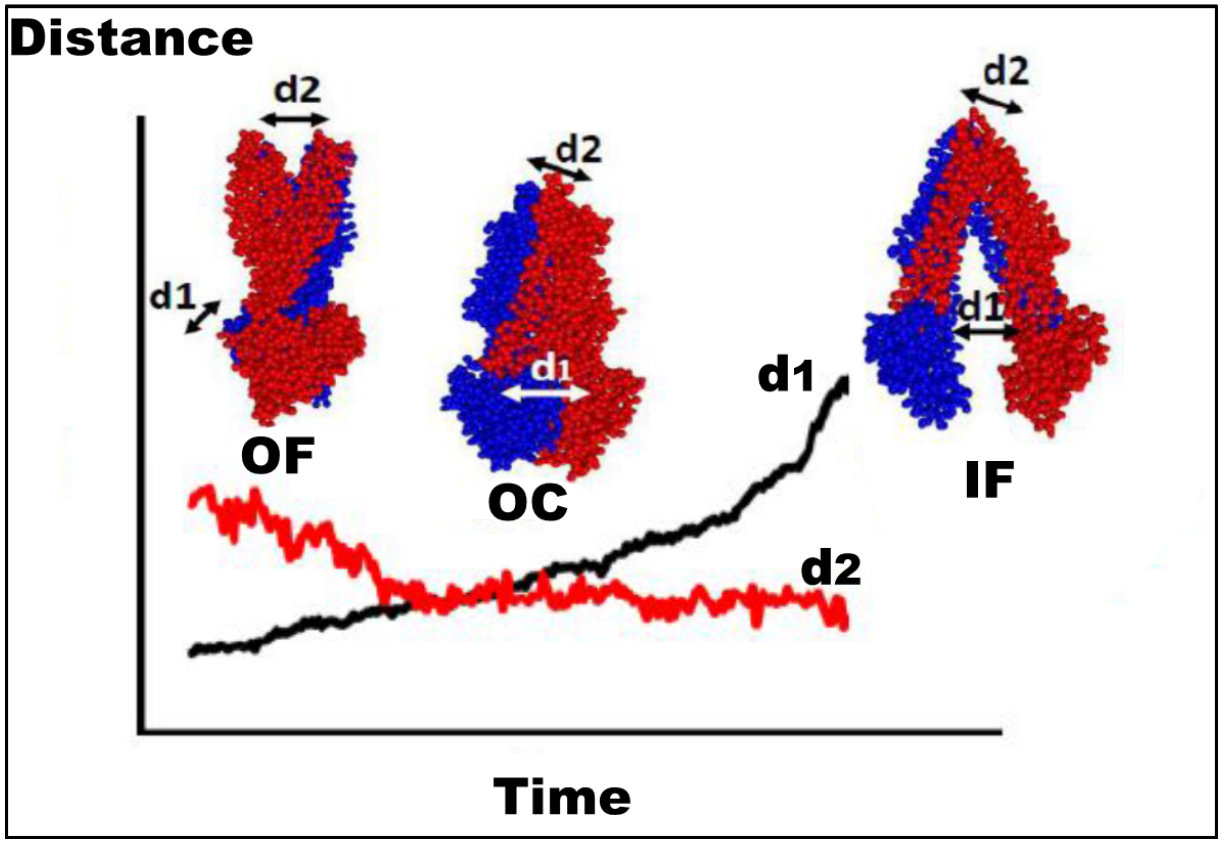

Nonequilibrium coarse-grained (CG) molecular dynamics (MD) simulations show that the ATP-binding cassette (ABC) exporter performs highly cooperative gating movements during the conformational transitions.

Public summary

- The CG-MD trajectory discloses highly cooperative gating movements in the MsbA ABC exporter protein.
- The potential mean force (PMF) is used to capture the conformational transitions between the OF, OC and IF states, and thus, a detailed understanding of the mechanism of ABC exporter gating is achieved at a molecular level.
- On the basis of the CG-MD simulation results, a mechanistic model, which is significantly different from those published in the literature, is proposed.

Citation: Wang Z, Liao J L. Molecular mechanism underlying ABC exporter gating: a computational study. *JUSTC*, **2023**, 53(12): 1207. DOI: 10.52396/JUSTC-2022-0134

JUSTC

Article

http://justc.ustc.edu.cn

Received: October 01, 2022; Accepted: November 04, 2022

Molecular mechanism underlying ABC exporter gating: a computational study

Zi Wang, and Jielou Liao ✉

Department of Chemical Physics, University of Science and Technology of China, Hefei 230026, China

✉Correspondence: Jielou Liao, E-mail: liaojl@ustc.edu.cn

Cite This: *JUSTC*, **2023**, 53(12): 1207 (6pp)

Read Online

SI Supporting Information

Abstract: ATP-binding cassette (ABC) exporters are a class of molecular machines that transport substrates out of biological membranes by gating movements leading to transitions between outward-facing (OF) and inward-facing (IF) conformational states. Despite significant advances in structural and functional studies, the molecular mechanism underlying conformational gating in ABC exporters is not completely understood. A complete elucidation of the state transitions during the transport cycle is beyond the capability of the all-atom molecular dynamics (MD) method because of the limited time scale of MD. In the present work, a coarse-grained molecular dynamics (CG-MD) method with an improved sampling strategy is performed for the bacterial ABC exporter MsbA. The resultant potential of the mean force (PMF) along the center-of-mass (COM) distances, d_1 and d_2, between the two opposing subunits of the internal and external gates, respectively, are obtained, delicately showing the details of the OF → IF transition occurring via an occluded (OC) state, in which the internal and external gates are both closed. The OC state has an important role in the unidirectionality of the transport function of ABC exporters. Our CG-MD simulations dynamically show that upon NBD dissociation, the opening of the internal gate occurs in a highly cooperative manner with the closure of the external gate. Based on our PMF calculations and CG-MD simulations in this paper, we proposed a mechanistic model that is significantly different from those recently published in the literature, shedding light on the molecular mechanism by which the ABC exporter executes conformational gating for substrate translocation.

Keywords: ATP-binding cassette exporter; potential of mean force; coarse-grained molecular dynamics; mechanistic model

CLC number: O643.1 **Document code:** A

1 Introduction

Adenosine 5′-triphosphate (ATP)-binding cassette (ABC) exporters are molecular machines that utilize the chemical energy from ATP to shuttle various substrates out of biological membranes[1,2]. ABC exporters are typified by two highly conserved nucleotide-binding domains (NBDs), which bind and hydrolyze ATP, and two transmembrane domains (TMDs) where a pathway for substrate translocation is formed (see Fig. 1). Whereas the NBDs are dimerized upon ATP binding, they depart from each other after ATP is hydrolyzed and the products are released. ABC exporters conduct important cellular functions via large-scale conformational changes by alternating between inward-facing (IF) and outward-facing (OF) conformations[3,4]. However, dysfunctional ABC exporters are responsible for several diseases, including adrenoleukodystrophy, pseudoxanthoma elasticum, cystic fibrosis, and cancer drug resistance[5]. Therefore, it is important to understand the molecular mechanism of ABC exporters to develop therapeutic agents against the abovementioned diseases.

An internal gate facing the cytoplasmic side (inward facing, IF) and an external gate facing the periplasmic side (outward facing, OF) are formed in the TMDs, each of which consists of six transmembrane helices (TMs) (labeled TM*i* and TM*i*′, *i*=1–6, in Fig. 1)[6]. Each TMD links its associated NBD with two intercellular coupling helices (ICH*s*, *s*=1, 2), ICH1 and ICH2 on one subunit and ICH1′ and ICH2′ on the other[6]. These ICHs are oriented roughly parallel to the membrane plane. The two gates are arranged roughly perpendicular to each other[7]. The internal gate consists of TM1, TM3, TM6, and the TM2-TM4′-TM5′ bundle on one side, and TM1′, TM3′, TM6′, and the TM2′-TM4-TM5 bundle on the opposite side (Fig. 1), whereas the external gate is composed of TM1, TM3′, TM6′, and the TM2-TM4′-TM5′ bundle on one side, and TM1′, TM3, TM6, and TM2′-TM4-TM5 on the other. Both gates share the TM2-TM4′-TM5′ and TM2′-TM4-TM5 bundles, which serve as two gateposts on each side of the gates, playing an important role in the semirigid-body gating movements of the protein. In an IF conformation, the external gate is closed, whereas the internal gate is open so that substrates can access from the cell interior, and vice versa in the OF state. In addition to the IF and OF states, the ABC exporter also adopts an occluded (OC) state, in which two gates are both closed.

Structural studies provide snapshots for conformational state transitions in ABC exporters[1,2]. Serving as a model system, the MsbA ABC exporter has been widely used to study the ABC exporter mechanism[8–12]. After the high-

DOI: 10.52396/JUSTC-2022-0134

JUSTC, **2023**, 53(12): 1207

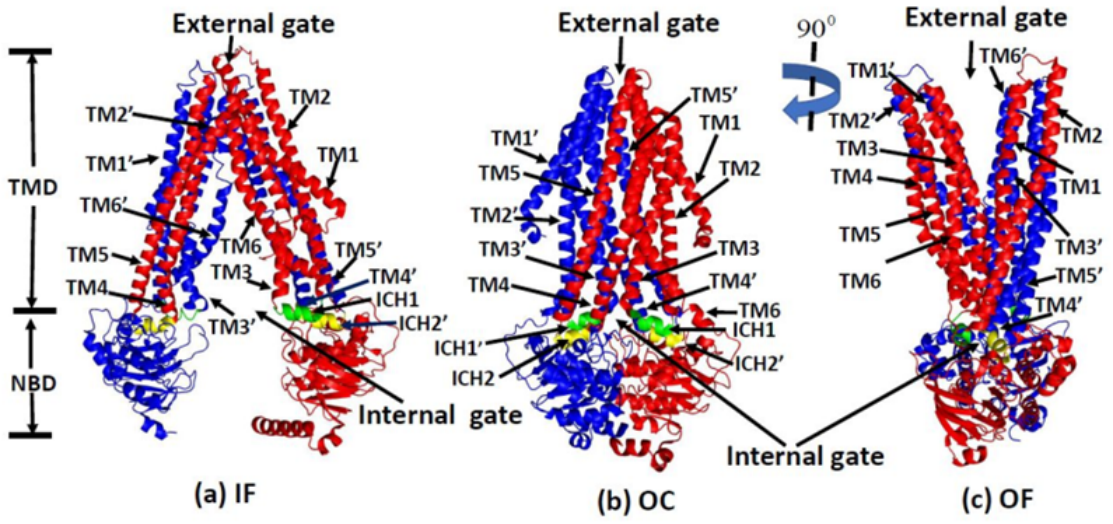

Fig. 1. Three conformations of an ABC exporter. (a) Inward-facing (IF) conformation, in which the internal gate is open whereas the external gate is closed. (b) Occluded (OC) conformation, in which both the internal and external gates are closed. (c) Outward-facing (OF) conformation, in which the internal gate is closed whereas the external gate is open. The TMD helices, TM1−TM6 on one subunit and TM1′−TM6′ on the other, are colored red and blue, respectively. The intracellular coupling helices ICH1 (ICH1′), which links TM2 (TM2′) and TM3 (TM3′) at its N- and C-terminus, and ICH2 (ICH2′), which links TM4 (TM4′) and TM5 (TM5′), are colored green and yellow, respectively.

resolution full-length X-ray structure was first determined for the Sav1866 ABC exporter in 2006[6], three MsbA crystal structures representing an OF state and two different IF states were reported from X-ray crystallography experiments[8]. Based on these MsbA structures, a mechanistic model (see Fig. S1 in Supporting information) was proposed, suggesting that the NBD twisting motion drives the alternation between the OF and IF states in the TMDs of MsbA[8]. This mechanistic model was derived from the highly twisted structures of MsbA in the IF states. Whether this model represents a general mechanism for ABC exporters remains controversial, as recent structural studies of MsbA have challenged this mechanistic view[9–11] (Figs. S1–S5). For example, a consensus model was suggested for conformational changes during the ABC transport cycle[2]. The proposed model follows steps similar to the classic alternating access between the OF and IF states[2]. However, the detailed mechanism in this meachistic model remains unclear (Fig. S3).

In principle, elucidating the conformational transition mechanism of an ABC exporter requires the evaluation of the free energy profile along the transition pathway (i.e., potential mean force, PMF)[13–15]. In an early study[14], Moradi and Tajkhorshid employed a nonequilibrium method to calculate the PMF for the conformational state transitions in MsbA. However, the PMF thus obtained was unable to capture the OF and OC states (see Fig. 5 in Ref. [14]). In other words, the PMF resulting from their modeling study captured the conformational transition only between the IF states of MsbA. In our previous paper[15], a coarse-grained molecular dynamics (CG-MD) method was used to obtain the PMF along the pathway for the ABC exporter conformational transitions. The resulting PMF can successfully elucidate the OF↔IF transitions. Unfortunately, it was unable to describe the OC state and therefore failed to capture the OF↔OC and OC↔IF state transitions. Despite extensive studies over the past decades, a detailed understanding of the molecular mechanism underlying ABC exporter gating remains incomplete[16]. To address this issue in this work, a CG-MD approach with comprehensive sampling is employed for the bacterial ABC exporter, MsbA.

2 Materials and methods

All simulations in this work were executed using GROMACS 5.0.5[17]. A full-length cryo-EM structure of MsbA (PDB code: 7RIT[13]) was used as the initial structure for our simulations. MsbA is the gram-negative bacterial ABC exporter that transports lipopolysaccharide (LPS), a potent inflammatory inducer, from the cytoplasmic leaflet to the periplasmic leaflet of the inner membrane[18]. As a member of the ABC exporter family, the structural architecture of MsbA is similar to that of other members, as described in the previous section. In this work, the POPC (1-palmitoyl-2-oleoyl-*sn*-glycero-3-phosphocholine) membrane system is employed. We used the Martini force field[19, 20] to model the MsbA molecule. The resulting CG model of MsbA was inserted into a preequilibrated POPC lipid bilayer also modeled with the Martini force field. In the Martini model, four water molecules are mapped to a CG water particle, and one ion is represented by a single CG ion particle. The MsbA-lipid system was solvated in the nonpolarizable Martini 2.2 model with 10% antifreeze-type water beads[21] and neutralized with 4 sodium ions in a rectangular box of 18 nm × 18 nm × 18 nm. The final system comprises 58379 MARTINI particles, including one MsbA protein (2452 particles), 987 POPCs, and 54940 nonpolarizable water CG particles (Fig. S1). The Martini model describes the van der Waals interactions with a Lennard–Jones potential function with a cutoff of 1.2 nm, which was smoothly shifted to zero between 0.9 and 1.2 nm, and treats charged CG particle interactions using a Coulomb energy function with a relative dielectric constant of 15. The long-range electrostatic interactions were treated using the particle mesh Ewald

DOI: 10.52396/JUSTC-2022-0134
JUSTC, **2023**, 53(12): 1207

(PME) method[22] with a real space cutoff of 1.2 nm and a 0.12 nm Fourier grid spacing. The Verlet scheme was used for the neighbor list update in accordance with the GROMACS definition.

CG-MD simulations were carried out using a time step of 20 fs under periodic boundary conditions. The MsbA-lipid system was weakly coupled to the v-rescale thermostat (τ_T = 1 ps) and the Parrinello−Rahman barostat (τ_p = 12 ps) fixed at 310 K and 1 bar in all simulations unless otherwise indicated. The total system was equilibrated after a 20000-step energy minimization. CG-MD simulations and umbrella sampling (US) with the weighted histogram analysis method (WHAM) were conducted to calculate the PMF along the transition pathway, which usually defines the reaction coordinate[15]. This reaction coordinate, which is used for monitoring the conformational changes in the protein, is critical for effective sampling of the conformations along the transition pathway. In Ref. [14], the angle between the roll axes of two sides of the internal gate, α, was used as the reaction coordinate to probe the conformational changes in the MsbA protein. It is helpful to use this angle for measuring the extent of the internal gating as a fully rigid body, but failing in the description of whether the gate is close or not in the case of MsbA, as it is a flexible protein but can perform semirigid body motion[23]. In a previous paper[15], the center-of-mass (COM) distance, d_1, between the two opposing subunits of the internal gate was applied as a reaction coordinate to sample the conformations along the transition pathway. The resulting PMF captures the OF↔IF transition but was not able to identify the OC state. In a recent publication[23], the difference between two COM distances, $d_1 - d_2$, was used as the reaction coordinate. Here, d_2 is the COM distance between the two opposing subunits of the external gate. Although the PMF was obtained, in which the OC state was identified, it is very difficult in practice to run the CG-MD trajectories along the reaction coordinate $d_1 - d_2$ (i.e., trajectories with the constraint to the reaction coordinate). To address this issue in this work, the COM distances d_1 and d_2 are used to investigate the dynamic correlation between these two gates during the conformational state transitions. To this end, a weak pulling force was used as a probe but only to the NBDs and a small portion of the TMDs at the cytoplasmic end of the internal gate. Consequently, the COM distances, d_1 and d_2, were gradually changed via successive pulling and equilibration steps. Structural snapshots were then taken out from the CG-MD trajectory to generate the configurations for the PMF simulations using the US method. Such a pulling approach has been widely applied to evaluate free energy profiles for various biological systems[25–27].

In this study, we first computed PMF vs the COM distance, d_1 (2.32–4.50 nm), along which 120 conformational windows were then generated. For each window, 60 ns CG-MD US simulations and WHAM were executed. The 60 ns CG-MD simulations for each window can achieve converged results, as also shown in our previous study[15]. To identify the OC state, we further took 60 configurations around the OF state from the above COM-pulling trajectory but performed US simulations along the d_2 direction (d_2: 2.40–2.90 nm). Therefore, we obtained the PMF against both d_1 and d_2 as the reaction coordinates (Fig. 2). The total effective simulation time[24] was ~46.8 μs in our calculations.

3 Results and discussion

3.1 Free energy profile along the conformational transition pathway

As discussed earlier, elucidation of the molecular mechanism of an ABC exporter needs to calculate the free energy profile along the transition pathway (i.e., potential mean force, PMF). In this work, both d_1 and d_2 are used as the reaction coordinates discussed above in our PMF calculations. Using the aforementioned methods, the PMF is thus obtained, as presented in Fig. 2.

As seen in Fig. 2, there exist several minima (a–d) corresponding to the OF, OC, IF_1, and IF_2 states, respectively. Here, IF_1 or IF_2 represents an IF state emerging at (c) or (d) in Fig. 2. The coarse-grained structures, which represent the OF (a), OC (b), IF_1 (c), and IF_2 (d) states, and their corresponding atomistic structures are obtained with the back mapping method[28], also shown in Fig. 2. The minimum point (a), where d_1=2.48 nm and d_2=2.83 nm, represents the OF state. Its alignment to the 2HYD structure[6] leads to a root-mean-squared deviation (RMSD) of 2.9 Å. The minimum point (b), d_1=2.61 nm and d_2=2.42 nm, identifies the OC state where the gates are both closed, while the minimum point (c), d_1=3.21 nm and d_2=2.39 nm, corresponds to an IF conformation (IF_1) with a 2.1 Å RMSD compared to the 5TV4 structure[9]. Intriguingly, the backbone of this IF_1 conformation is similar to that of the heterodimeric ABC exporter TM287/TM288 (PDB code: 3QF4[29]) (RMSD of 3.5 Å for Cα atoms). The deepest basin (d) is found in the range of d_1 from 3.48 to 3.82 nm, and d_2=2.34 nm represents IF_2 states, whose conformations resemble a number of ABC exporter structures from experiments, including the 7RIT[13] and 4F4C[30] structures. Overall, the free energy of the OF state is relatively higher than that of

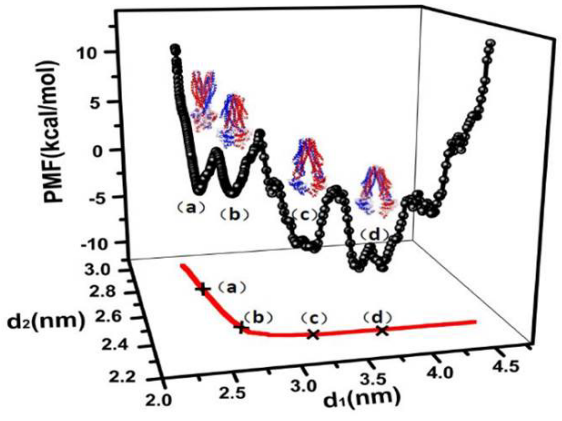

Fig. 2. Potential of mean force (PMF) expressed as a function of the COM distances, d_1, for the internal gate, and d_2, for the external gate. (a) d_1=2.48 nm and d_2=2.83 nm, (b) d_1=2.61 nm and d_2=2.42 nm, (c) d_1=3.21 nm and d_2=2.39 nm, and (d) d_1=3.48–3.82 nm and d_2=2.34 nm represent the OF, OC, IF_1, and IF_2 states, respectively. The coarse-grained structures, which represent the (a) OF, (b) OC, (c) IF_1, and (d) IF_2 states, and their corresponding atomistic structures are also presented.

DOI: 10.52396/JUSTC-2022-0134
JUSTC, **2023**, 53(12): 1207

an IF state in the absence of nucleotides, consistent with experimental observations[16]. We anticipate that the tight binding of ATP would lower the OF free energy basin and make the OF state more stable.

Our PMF calculations demonstrate that the OC conformation represents a stable state (see (b) in Fig. 2), in agreement with structural and biochemical experiments[2,4]. The resulting PMF shows that the OF IF transition must proceed via the OC state. This finding is important for the unidirectionality of the transport function of an ABC exporter, as the external state needs to be closed before the internal gate is open. Otherwise, if the internal and external gates were both open, it might cause reverse transport of substrates through the membrane by the ABC exporter.

As shown in Fig. 2, during the OF→OC transition, d_2 is decreased by 4.1 Å, whereas d_1 is increased by only 1.3 Å. As the free energies still change abruptly within this small distance range of d_1, it would be difficult to describe the detailed PMF changes by including the OC state during the OF→OC transition using only d_1 as the reaction coordinate. This may offer a rationale for why the PMF fails in the description of the OC state in our previous study[15]. As the calculated PMF provides only a static picture, it is of great interest to probe how the coordinated gating movements are achieved dynamically during the MsbA state transitions. To this end, the trajectories from our CG-MD simulations will be analyzed in detail as follows.

3.2 Highly cooperative dynamics in the MsbA gating movements revealed by CG-MD simulations

NBD dissociation triggers a series of conformational transitions, leading to the closure of the external gate and the opening of the internal gate in the ABC exporter. In the following discussion, the variations in the COM distances d_{NBD}, d_1, and d_2 are used to monitor the dissociation of two NBDs and the movements of the internal and external gates, respectively. The COM distances d_{ICH1} and d_{ICH2} are also presented to depict the time courses of the COM distances between ICH1 and ICH1′ and between ICH2 and ICH2′, respectively. These two pairs are inserted into the respective NBD, allowing the TMD to bind to the NBD together.

As shown in Fig. 3, d_{NBD} (blue line) increases slowly in the early phase of NBD dissociation, as the two NBDs are associated tightly with each other in the OF state. The COM distances d_{ICH1}, d_{ICH2} and d_1 rise in a way similar to that of d_{NBD}. The results show that the dissociation of the NBDs drives the internal gate to be opened with ICHs and ICHs′ (s=1, 2) that couple the TMDs to the NBDs.

As shown in Fig. 3, d_2 descends gradually as d_1 ascends, demonstrating that the closing of the external gate occurs in a highly cooperative way with the opening of the internal gate. In Fig. 3, the cross point of the d_1 (black) and d_2 (red) curves, where d_1= d_2=2.5 nm, corresponds to the OC state, in which both gates are closed (see Fig. 2). After this time point, the d_1 curve continues to go upward to a point, where d_1=3.2 nm and d_2=2.4 nm, corresponding to the IF_1 state, where the external gate is closed and the internal gate is already open. Our CG-MD simulations dynamically capture the OC state during the OF→IF state transition.

The high degree of cooperativity in the gating movements of the ABC exporter relies on the protein structure. As first determined in the X-ray experiment[6], the ABC exporter structures are characterized by a domain-swapped arrangement, i.e., TM4 and TM5 in one subunit reach across and contact the NBD in the other subunit (Fig. 1). Therefore, TM4 and TM5 (TM4′ and TM5′) in one subunit are allowed to interact tightly with TM2′ (TM2) in the other subunit, forming a rather rigid TM4-TM5-TM2′ (TM4′-TM5′-TM2) bundle. As mentioned earlier, these two bundles serve as two movable but rigid gateposts shared by the internal and external gates, which are arranged approximately perpendicular to each other (Fig. 1). Such a mechanical arrangement enables the protein to perform machine-like functions in a highly cooperative way. Therefore, a mechanistic model is proposed for conformational state transitions in the ABC exporter in the following discussion.

3.3 Mechanistic model for conformational state transitions in the ABC exporter

To probe the mechanism underlying the conformational state transition of the MsbA exporter, several coarse-grained structures are taken out from the CG-MD trajectory, displayed in Fig. 2.

These structures correspond to the (a) OF, (b) OC, (c) IF_1, and (d) IF_2 states. For clarity, only TM3 (TM3 ′), TM4 (TM4′), TM5 (TM5′), and the NBDs are retained, as presented in Fig. 4A. The two subunits are presented as red and blue solid balls, respectively. As shown in Fig. 4, TM3, TM4 and TM5 with an NBD from one subunit are colored red, and TM3′, TM4′ and TM5′ with another NBD from the other subunit are colored blue. As shown in Fig. 4A(d) as well as Fig. 4B(d), while TM3 (TM3 ′) inserts the red NBD (blue NBD), TM4-TM5 (TM4 ′-TM5 ′) crossover and inserts the other blue (red) NBD. This outstanding domain-swapped feature distinguishes an ABC exporter from an ABC importer[6], playing an important role in the ABC exporter machinery.

Corresponding to Fig. 4A, a mechanistic model is constructed for the transitions between the OF, OC, IF_1, and IF_2 states,

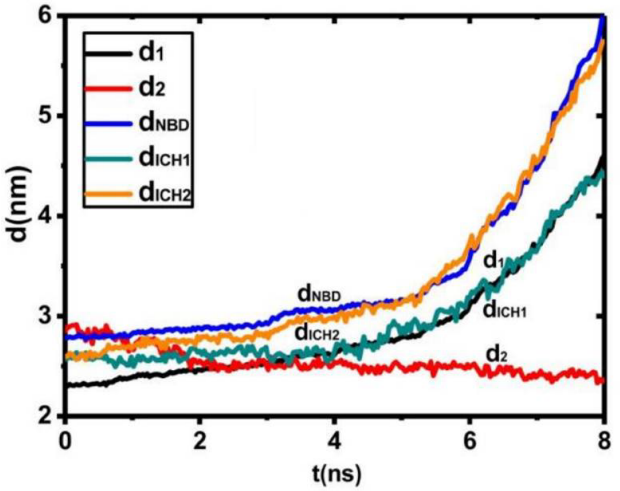

Fig. 3. Time evolution of d_1, d_2, d_{NBD}, d_{ICH1} and d_{ICH2} upon NBD dissociation.

DOI: 10.52396/JUSTC-2022-0134
JUSTC, **2023**, 53(12): 1207

depicted in Fig. 4B. As elucidated in this mechanistic model, starting from the OC state (a), NBD dissociation, which usually occurs upon ATP hydrolysis and the release of the products from an ABC transporter[31], drives the TM4-TM5-TM2′ bundle (TM2′ and TM2 not shown in Fig. 4) on one subunit (blue) to gradually depart from its counterpart, i.e., the TM4′-TM5′-TM2 bundle on the other (red). Therefore, mechanical force is generated by the NBD dissociation to close the external gate, leading to the transition from the OF to OC state (step 1, Fig. 4B). As the NBDs depart from each other further, the internal gate is open, resulting in the IF_1 state (step 2). The two NBDs continue to dissociate from each other, and the IF_2 state emerges with the internal gate more open and the external gate closer (step 3). The OF→IF transition occurs, and the IF_2 state is eventually reached. Following a procedure similar to that in our previous study[15], the above steps shown in Fig. 4 can be performed in reverse by applying weak forces to push the NBDs to approach each other, mimicking NBD association in the presence of ATP. As such, one cycle for the conformational state transitions in the ABC exporter is completed.

The above mechanistic model for the ABC export machinery is proposed based on our PMF and CG-MD simulations, demonstrating how the external gate is closed in response to the opening of the internal gate upon NBD dissociation. As shown in Fig. 4, the movement direction of the external gate is approximately perpendicular to that of the internal gate. This is consistent with the structural arrangement discussed earlier, showing the structural basis for the model. Our machinestic model is significantly different from those popular ones presented in recent publications[2–4, 9–13] (Figs. S2–S5). Unfortunately, the overwhelming majority of those models do not capture the domain-swapped structural feature of ABC exporters, thereby failing to elucidate the detailed molecular mechanism underlying conformational gating in ABC exporters.

4 Conclusions

ABC exporters extrude various substrates out of the cell membrane through dynamic switching between the OF and IF conformations via the OC state. However, a detailed understanding of the molecular mechanism underlying conformational gating in ABC exporters currently remains incomplete.

In the present study, we used the combined CG-MD method with an improved sampling approach to study the bacterial ABC exporter MsbA. The resulting PMF identified the pathway for the conformational transitions between the OF, OC, and IF states. The OF, OC IF_1 and IF_2 structures obtained from the CG-MD and PMF simulations are in agree-

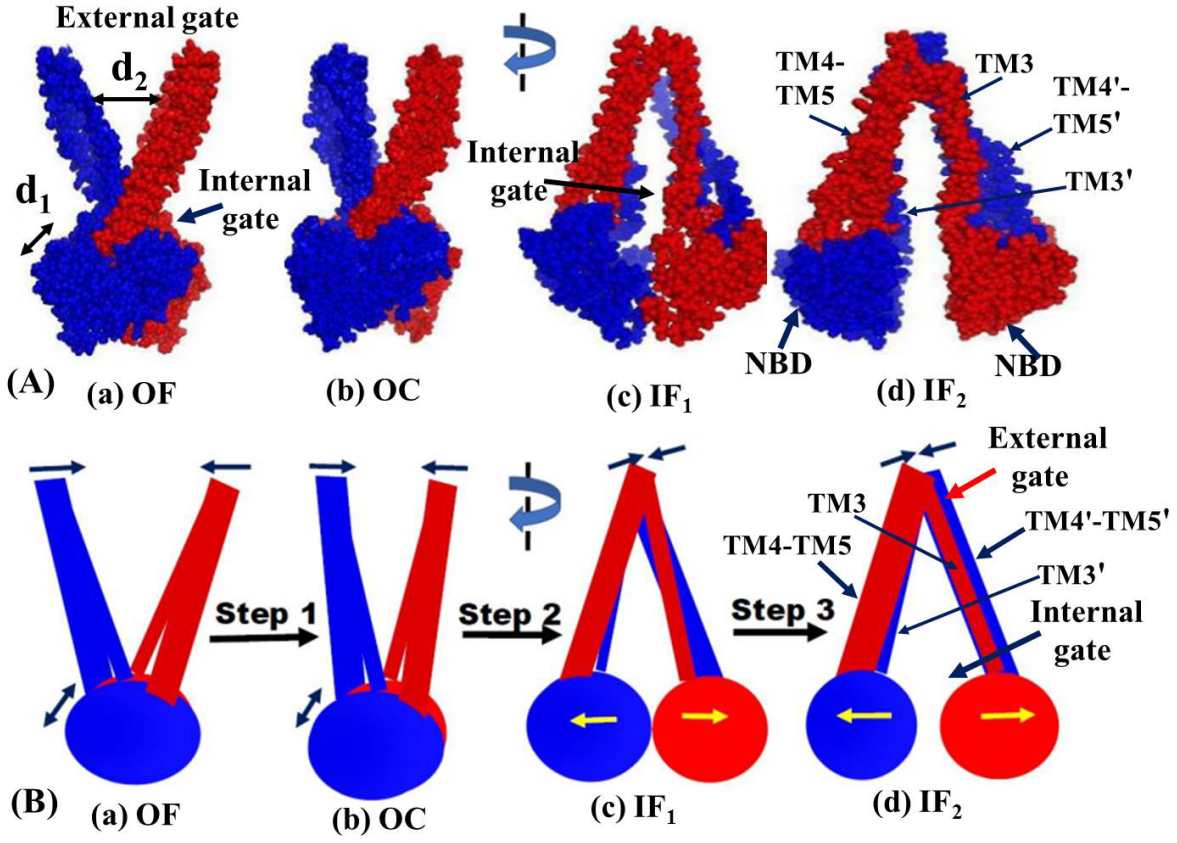

Fig. 4. (A) Coarse-grained structures from the CG-MD simulations for the (a) OF, (b) OC, (c) IF_1, and (d) IF_2 states and (B) a mechanistic model for conformational state transitions in response to NBD dissociation. For clarity, two NBDs are presented with two balls (red and blue), and only TM3 and TM4-TM5 (red) and TM3′ and TM4′-TM5′ (blue) are presented with rectangular sticks. The COM distances d_1 and d_2 are displayed in (A). In (B), the wider rectangular sticks represent TM4-TM5 (red, TM2′ not shown) and TM4′-TM5′ (blue, TM2 not shown), whereas the narrower rectangular sticks represent TM3 (red) and TM3′ (blue). In (B), symbols ↔ and ←→ represent the gate opening, whereas →← represents the closing of a gate.

DOI: 10.52396/JUSTC-2022-0134
JUSTC, **2023**, 53(12): 1207

ment with the structural experiments. Our simulations show that in response to NBD dissociation, the closing of the external gate is highly cooperative with the opening of the internal gate. The results demonstrate that the closure of the external gate occurs prior to the opening of the internal gate so that the OC state is captured in both the PMF and CG-MD simulations in this work. This is functionally important for the transport unidirectionality of an ABC exporter. Otherwise, a conformation in which the internal and external gates were both open could occur, causing reverse transport of substrates via an ABC exporter across the membrane. Based on our PMF and CG-MD simulations in this work, a mechanistic model is proposed for the ABC export machinery, shedding light on the molecular mechanism underlying conformational gating in the ABC exporter.

Supporting informaion

The supporting information for this article can be found online at https://doi.org/10.52396/JUSTC-2022-0134.

Acknowledgements

This work was supported by the National Natural Science Foundation of China (21073170, 21273209).

Conflict of interest

The authors declare that they have no conflict of interest.

Biographies

Zi Wang received his Ph.D. degree in Chemistry from the University of Science and Technology of China. He is currently a senior engineer in biochemical research and development at the BGI Research, Shenzhen. His research mainly focuses on protein design and directed evolution of enzymes.

Jielou Liao is a Professor in Physical Chemistry at the University of Science and Technology of China. His current research interests include theoretical and computational biology and chemistry as well as quantum biology.

References

[1] Thomas C, Tampé R. Structural and mechanistic principles of ABC transporters. *Annu. Rev. Biochem.*, **2020**, *89*: 605–636.
[2] Srikant S, Gaudet R. Mechanics and pharmacology of substrate selection and transport by eukaryotic ABC exporters. *Nat. Struct. Mol. Biol.*, **2019**, *26* (9): 792–801.
[3] Hofmann S, Januliene D, Mehdipour A R, et al. Conformation space of a heterodimeric ABC exporter under turnover conditions. *Nature,* **2019**, *571* (7766): 580–583.
[4] Locher K P. Mechanistic diversity in ATP-binding cassette (ABC) transporters. *Nat. Struct. Mol. Biol.*, **2016**, *23* (6): 487–493.
[5] Robey R W, Pluchino K M, Hall M D, et al. Revisiting the role of ABC transporters in multidrug-resistant cancer. *Nat. Rev. Cancer,* **2018**, *18* (7): 452–464.
[6] Dawson R J P, Locher K P. Structure of a bacterial multidrug ABC transporter. *Nature,* **2006**, *443* (7108): 180–185.
[7] Dawson R J P, Locher K P. Structure of the multidrug ABC transporter Sav1866 from Staphylococcus aureus in complex with AMP-PNP. *FEBS Lett.*, **2007**, *581* (5): 935–938.
[8] Ward A, Reyes C L, Yu J, et al. Flexibility in the ABC transporter MsbA: Alternating access with a twist. *Proc. Natl. Acad. Sci. U.S.A.,* **2007**, *104* (48): 19005–19010.
[9] Mi W, Li Y, Yoon S H, et al. Structural basis of MsbA-mediated lipopolysaccharide transport. *Nature,* **2017**, *549* (7671): 233–237.
[10] Ho H, Miu A, Alexander M K, et al. Structural basis for dual-mode inhibition of the ABC transporter MsbA. *Nature,* **2018**, *557* (7704): 196–201.
[11] Padayatti P S, Lee S C, Stanfield R L, et al. Structural insights into the lipid A transport pathway in MsbA. *Structure,* **2019**, *27* (7): 1114–1123.e3.
[12] Angiulli G, Dhupar H S, Suzuki H, et al. New approach for membrane protein reconstitution into peptidiscs and basis for their adaptability to different proteins. *eLife,* **2020**, *9*: e53530.
[13] Thélot F A, Zhang W, Song K, et al. Distinct allosteric mechanisms of first-generation MsbA inhibitors. *Science,* **2021**, *374* (6567): 580–585.
[14] Moradi M, Tajkhorshid E. Mechanistic picture for conformational transition of a membrane transporter at atomic resolution. *Proc. Natl. Acad. Sci. U.S.A.,* **2013**, *110* (47): 18916–18921.
[15] Wang Z, Liao J L. Probing structural determinants of ATP-binding cassette exporter conformational transition using coarse-grained molecular dynamics. *J. Phys. Chem. B,* **2015**, *119* (4): 1295–1301.
[16] Kieuvongngam V, Chen J. Structures of the peptidase-containing ABC transporter PCAT1 under equilibrium and nonequilibrium conditions. *Proc. Natl. Acad. Sci. U.S.A.,* **2022**, *119* (4): e2120534119.
[17] Abraham M J, Murtola T, Schulz R, et al. GROMACS: High performance molecular simulations through multi-level parallelism from laptops to supercomputers. *SoftwareX,* **2015**, *1–2*: 19–25.
[18] Simpson B W, Trent M S. Pushing the envelope: LPS modifications and their consequences. *Nat. Rev. Microbiol.,* **2019**, *17* (7): 403–416.
[19] Marrink S J, Risselada H J, Yefimov S, et al. The MARTINI force field: Coarse grained model for biomolecular simulations. *J. Phys. Chem. B,* **2007**, *111* (27): 7812–7824.
[20] Monticelli L, Kandasamy S K, Periole X, et al. The MARTINI coarse-grained force field: Extension to proteins. *J. Chem. Theory Comput.,* **2008**, *4* (5): 819–834.
[21] López C A, Sovova Z, van Eerden F J, et al. Martini force field parameters for glycolipids. *J. Chem. Theory Comput.,* **2013**, *9* (3): 1694–1708.
[22] Darden T, York D, Pedersen L. Particle mesh Ewald: An $N\cdot\log(N)$ method for Ewald sums in large systems. *J. Chem. Phys.,* **1993**, *98*: 10089–10092.
[23] Huang Y, Xu H C, Liao J L. Coarse-grained free-energy simulations of conformational state transitions in an adenosine 5′-triphosphate-binding cassette exporter. *Chin. J. Chem. Phys.,* **2020**, *33*: 712–716.
[24] Periole X, Knepp A M, Sakmar T P, et al. Structural determinants of the supramolecular organization of G protein-coupled receptors in bilayers. *J. Am. Chem. Soc.,* **2012**, *134* (26): 10959–10965.
[25] Lemkul J A, Bevan D R. Assessing the stability of Alzheimer's amyloid protofibrils using molecular dynamics. *J. Phys. Chem. B,* **2010**, *114* (4): 1652–1660.
[26] Jakubec D, Vondrášek J. Efficient estimation of absolute binding free energy for a homeodomain-DNA complex from nonequilibrium pulling simulations. *J. Chem. Theory Comput.,* **2020**, *16* (4): 2034–2041.
[27] Xing X, Liu C, Ali A, et al. Novel disassembly mechanisms of sigmoid $A\beta_{42}$ protofibrils by introduced neutral and charged drug molecules. *ACS Chem. Neuro.,* **2020**, *11* (1): 45–56.
[28] Wassenaar T A, Pluhackova K, Böckmann R A, et al. Going backward: A flexible geometric approach to reverse transformation from coarse grained to atomistic models. *J. Chem. Theory Comput.,* **2014**, *10* (2): 676–690.
[29] Hohl M, Briand C, Grütter M G, et al. Crystal structure of a heterodimeric ABC transporter in its inward-facing conformation. *Nat. Struct. Mol. Biol.,* **2012**, *19* (4): 395–402.
[30] Jin M S, Oldham M L, Zhang Q, et al. Crystal structure of the multidrug transporter P-glycoprotein from *Caenorhabditis elegans*. *Nature,* **2012**, *490* (7421): 566–569.
[31] Huang W, Liao J L. Catalytic mechanism of the maltose transporter hydrolyzing ATP. *Biochemistry,* **2016**, *55* (1): 224–231.

DOI: 10.52396/JUSTC-2022-0134
JUSTC, **2023**, 53(12): 1207